



## Parametric stress-strain analysis for upstream slope of the asphaltic concrete core rockfill dams in static state

### Análisis paramétrico de esfuerzo-deformación para la pendiente superior de presas de núcleo de relleno de roca de hormigón asfáltico en estado estático

Shahram Shiravi\*, Arash Razmkhah

Department of Civil Engineering, South Tehran Branch, Islamic Azad University, Tehran, Iran.

\* Corresponding author email: [shahram\\_shiravi@yahoo.com](mailto:shahram_shiravi@yahoo.com)

(*recibido/received: 18-octubre-2021; aceptado/accepted: 02-diciembre-2021*)

#### ABSTRACT

In this study, the effects of various geometric parameters of a dam in 2D static analysis of stress-strain on the upstream slope of the asphaltic concrete core rockfill dams were investigated. For this purpose, first, the geometric characteristics of a large number of the world's dams were collected and assessed, then by geometric modeling of these dams, many numerical models were developed for static analysis using GeoStudio software in eight height classes, three cases of upstream and downstream slopes, three different shapes and thickness of the asphaltic concrete core under different Impounding states including "Full Reservoir", "Half full Reservoir", "End of construction and "Rapid Drawdown on a rigid type of foundation. The results of this study demonstrated that in four different construction and impounding states and in three different cases of slopes, Increasing the height parameter, causes increasing the Maximum total stress, Maximum total strain, Shear strain, and Maximum shear stress for all construction and impounding states. The Maximum total stress decreased for all operating situations as the upstream slope reduced. According to the obtained results from the static stress-strain analysis, increasing both vertical and inclined asphaltic concrete core thicknesses leads to decreasing the Maximum shear stress in the Full Reservoir state but it increases in other states of impoundment. Moreover, by comparing the displacements related to specified points on the upstream slopes, increasing the height parameter, leads to increasing both horizontal and vertical displacements, the volumetric strain, deviator strain, and deviator stress for all impounding conditions. In the following, the additional results were provided along with diagrams for further analysis.

**Keywords:** Asphaltic Concrete Core, Shear Stress, Static Analysis, Shear Strain, Rockfill Dam, Rapid Drawdown, Boundary Condition.

#### RESUMEN

En este estudio, se investigaron los efectos de varios parámetros geométricos de una presa en el análisis estático 2D de tensión-deformación en la pendiente aguas arriba de las presas de relleno de roca con núcleo de concreto asfáltico. Para ello, primero se recopilaron y evaluaron las características geométricas de una gran cantidad de presas del mundo, luego mediante el modelado geométrico de estas presas, se desarrollaron muchos modelos numéricos para análisis estático utilizando el software GeoStudio en ocho clases de altura,

tres casos de aguas arriba y aguas abajo pendientes, tres formas y espesores diferentes del núcleo de concreto asfáltico bajo diferentes estados de incautación, incluyendo "Reservorio lleno", "Reservorio medio lleno", "Fin de la construcción y" Descenso rápido en un tipo rígido de cimentación. Los resultados de este estudio demostraron que en cuatro estados de construcción y embalses diferentes y en tres casos diferentes de taludes, el aumento del parámetro de altura provoca un aumento de la tensión total máxima, la tensión total máxima, la deformación cortante y el esfuerzo cortante máximo en todos los estados de construcción y embalse. La tensión total máxima disminuyó en todas las situaciones operativas a medida que se redujo la pendiente aguas arriba. De acuerdo con los resultados obtenidos del análisis de tensión-deformación estática, el aumento de los espesores del núcleo de hormigón asfáltico tanto vertical como inclinado conduce a una disminución del esfuerzo cortante máximo en el estado de depósito lleno, pero aumenta en otros estados de embalse. Además, al comparar los desplazamientos relacionados con puntos especificados en las pendientes aguas arriba, el aumento del parámetro de altura conduce a un aumento de los desplazamientos horizontales y verticales, la deformación volumétrica, la deformación del desviador y la tensión del desviador en todas las condiciones de embalse. A continuación, se proporcionaron los resultados adicionales junto con diagramas para un análisis más detallado.

**Palabras claves:** Núcleo de hormigón asfáltico, Esfuerzo cortante, Análisis estático, Deformación cortante, Presa de relleno de roca, Reducción rápida, condición de contorno.

## 1. INTRODUCTION

Despite the passage of thousands of years of the dam industry, the design of dams, especially Rockfill and Embankment dams, is still based on taste and initiative. However, this initiative must be approved by scientific standards and criteria. With the ever-increasing soil mechanics science over the past, many dam construction activities to be codified within the framework of scientific law. Nowadays, the development of instrumentation and measurement techniques on the one hand, and the development of computational and analytical solutions, on the other hand, have contributed to the fundamental perspectives on understanding the behavior of dams and clarified pathways to study. So that the various types of dams are constructed and operated in accordance with the climatic conditions and geography of the given regions. The use of Central or Inclined asphaltic concrete core for Rockfill and embankment dams all over the world, especially in Europe, has become the most popular and reliable method for experts in this field. Asphaltic concrete diaphragm, in addition to stability, also provides a suitable sealing coat. The advantages of using the diaphragm mentioned above in Rockfill dams have made it a reasonable alternative instead of clay core in many cases. Despite all the advantages of these dams, it is still important to study, analyze and understand the static and dynamic behaviors of these structures, especially at critical points.

## 2. BACKGROUND OF THE STUDY

Valstad et al. studied the Storvatn Dam with 90m high in Norway and using the Newmark method, showed that in severe earthquakes, the thin asphaltic concrete diaphragms in some areas near the crest of the dam were damaged and cracked (Valstad et al., 1992).

Hoeg also conducted a study on the Storvatn Dam and found that if the dam slopes were very steep, large shear strains might develop at the top of the dam's asphalt concrete core. He also demonstrated that rockfill dams with asphalt concrete cores had enough resistance to withstand earthquakes (Höeg, 1993). Mahinroosta studied a 115m high asphaltic concrete core rockfill dam against expected seismic events using the Newmark method, both the linear Mohr-Coulomb (MC) criterion and Nonlinear MC criterion via Flac2D software. The thickness of the asphaltic concrete core was 1m, the width of the transition zone was 3m, the upstream and downstream slopes were 1V:1.6H and the foundation was placed on a high-strength rock layer. The results show that the acceleration value of the dam crest in the equivalent-linear analysis was higher

than that in Nonlinear analysis. The plastic deformation was observed in the asphaltic concrete core and transition zones, but the shear strain in the filter material was much higher than in the asphaltic core. An increase was observed in shear and volumetric strains near the dam crest during dynamic analysis, leading to the deformation of the asphaltic concrete core for the upstream slope. The acceleration value of Nonlinear analysis is also less than equivalent-linear analysis. In Nonlinear analysis, the amount of slip was observed at top of the asphaltic concrete core for the dam's upstream side. Also, in both equivalent-linear analysis and Nonlinear analysis, an increase in cracking was observed at the top of the asphaltic concrete core (Mahinroosta).

Ziaei Moayed and Fatemi conducted a study on the Gabrik dam located in Hormozgan province with a height of 41m on a 13m thick bed of the alluvium by using the FEADAM 84 which is a Finite Element software for Analysis of Dams. In the research, both the linear behavior of the core materials and the Nonlinear behavior of other materials were considered and the static analysis was carried out using the finite element method. The results showed that in various states, the values of horizontal strain in core elements were less than 1.2%. Therefore, it is predicted that the asphaltic core after deformation remains impermeable. Due to the shear stresses observed in the core, the probability of shear rupture in the core elements was low. By increasing the core stiffness, the maximum principal stress was increased in the depth of the core, indicating that more stress is absorbed by the asphaltic concrete core (Moayed et al., 2001).

Feizi, Mirghasemi, and Ghanooni considering the shape of different valleys examined a dam with 30m height and 1m thick asphalt concrete core along with the same upstream and downstream slopes on bedrock by Flac3D software. The models mentioned above were statically and dynamically analyzed in both construction and impounding conditions based on the Mohr-Coulomb model to calculate the values of displacements and stresses. The obtained results showed that at the end of construction, while the maximum settlement occurred on both sides of the asphalt concrete core, in most cases, the asphalt core could not have much effect on the overall behavior of the dam. Also, due to the relative symmetry that occurred in these conditions, the shear stresses near the asphalt concrete core were zero. But in the state of the full reservoir, water was applied directly to the core, which could increase the horizontal settlement in the lower part of the shell. In dynamic analysis, the maximum settlement occurred near the dam crest (Feizi et al., 2005).

Baziar, Salemi, and Heidari investigated the seismic behavior of the Meyjaran asphalt concrete core dam constructed in Northern Iran, with 60m height and 180m crest length based on materials obtained from laboratory tests.

Nonlinear numerical analysis was performed by using the FLAC 3D finite-difference software at different earthquake levels. Studies showed that the elastoplastic characteristics of asphalt concrete core behave satisfactorily during earthquake loading. The asphaltic core remains waterproof during an earthquake with  $a_{max}=0.25g$ . However, during an earthquake with  $a_{max}=0.60g$ , some cracks may occur towards the core top zone and below the crest thus the core permeability increases but the dam would still be safe (Baziar et al., 2006).

Gatmiri and Mokarram employed the ADINA software to perform linear and nonlinear dynamic analysis on samples of the asphalt concrete core embankment dams for all construction and impounding stages. In order to determine the sensitivity of the analysis to geometric parameters, by steeping the slopes and doubling the height of the models, they concluded that it is necessary to design, select the slopes and the final height of the dam based on the exact seismic behavior of the dam at different heights and slopes. Also, the most important factor influencing the instability of the dam in the dynamic analysis was the height parameter. In addition, they found that the asphalt concrete core can withstand temporary and permanent

displacements without the occurrence of hydraulic cracking in the core or uncontrolled water leakage (Gatmiri & Mokarram, 2003).

Razmkhah and Shiravi performed the static slope stability analysis on several numerical models with different asphaltic concrete core shapes for a wide range of different geometrical parameters in different construction and impounding stages. They concluded that the safety factor of the upstream and downstream slopes reduced as the dam's height increased at a constant slope. The End of Construction stage has the Maximum stability safety factor after the Full Reservoir stage. Also in the Rapid Drawdown stage, for all dam heights and slopes, the upstream slope stability is less than the downstream slope (Razmkhah & Shiravi, 2016).

### 3. PURPOSE OF THE STUDY

In this study, the static stress-strain analysis was performed for all models in different stages of "End of Construction", "Full Reservoir", "Half Full Reservoir" and "Rapid Drawdown", which aimed to obtain the maximum values of Total Stress, Total Strain, Shear Stress and Shear Strain, Volumetric and Deviator Strains, Horizontal and Vertical Displacements and Deviator Stress in given points, including the beginning, middle and ending zones of the dam upstream slope. Also, to evaluate the behavior of the models, comparative diagrams for the values mentioned above was reported.

The constraints status and impounding stages of dams were assigned to all models as the boundary conditions. For this purpose, SIGMA/W was used based on the finite element method. SIGMA/W is a powerful finite element software product which provides acceptable analytical practice for all projects and its results can be used in many major engineering activities such as dam industry, tunneling, etc. It is used by many experts across the world in various fields of research, etc. (Ltd., 2010).

#### 3.1. Dam height

The height of a dam represents the vertical distance from the lowest point of natural ground on the dam's downstream side to the dam crest. In this study, the height parameter was selected to cover an acceptable range of height in modeling. For this purpose, as shown in Table 1, the models were grouped into eight height classes. Given that all the models selected in this study had the same height or more than 50 meters, all models were considered large dams according to the definition of the International Commission on Large Dams (ICOLD).

Table 1. Dams specifications for modeling and analysis (Razmkhah et al., 2016)

| Country        | Rockfill Dam Name | Real Height (m) | Height Class | Country   | Rockfill Dam Name | Real Height (m) | Height Class |
|----------------|-------------------|-----------------|--------------|-----------|-------------------|-----------------|--------------|
| United Kingdom | Megget            | 56              | 50           | Hong Kong | High Island West  | 95              | 90           |
| Norway         | Berdalsvatn       | 65              | 60           | Canada    | La Romaine 2      | 110             | 110          |
| Germany        | Schmalwasser      | 76              | 70           | Norway    | Storgolmvatn      | 125             | 125          |
| Macedonia      | Zletovica         | 85              | 80           | China     | Quxue             | 170             | 170          |

#### 3.2. Dam crest width and Freeboard

The freeboard of a dam is a suitable depth to compensate for increasing wave height in the slope of the body, and cope with the wave height due to wind and possible changes in design flood estimation, which represents the vertical distance between the dam crest and the highest reservoir water level in the worst flooding. In this study, based on the criteria of ICOLD, for ease of calculation and modeling, the width equal to 5m

was assigned to all numerical models. Also, the dam crest width, which provided the conditions for the transport of vehicles, had a minimum width of 4m according to various technical recommendations. However, it is often considered wider in designs for greater strength against slippage and the effects of earthquakes. In this regard, as shown in Table 2, the mentioned width was assigned to the models in accordance with each height class.

Table 2. Crest widths of dams behavioral models (Razmkhah et al., 2016).

| Height Class        | 50  | 60  | 70  | 80  | 90  | 110 | 125 | 170 |
|---------------------|-----|-----|-----|-----|-----|-----|-----|-----|
| Dam Crest Width (m) | 9.5 | 7.0 | 8.0 | 8.5 | 9.5 | 6.0 | 7.0 | 9.5 |

### 3.3. Foundation depth

In this discussion, all numerical models were modeled on a bedrock foundation, assuming fixed support. To facilitate modeling, it was necessary to cut out the foundation edges of their sides for all the models. For this purpose, in order to make the modeling closer to reality and continuously define the foundation on both sides of the dam, the elements located at the foundation edge of the behavioral models become infinite. In this way, the mentioned elements are to be continuous from the right to the positive infinity, and on the other side, the elements continue to the negative infinity (Ltd, 2010). The sealing process of the foundation is accomplished by grout injection (Grout curtain method) to a depth equal to one-third of the dam height or at least 10m below the bedrock surface (Kjaernsli, 1991). According to the cases mentioned in this section, foundation depths are approximately equal to one-third of the dam height for all models.

Table 3. Foundation depths for dam models in proportion to each height class

| Height Class | Foundation Depth (m) |
|--------------|----------------------|
| 50           | 15                   |
| 60           | 20                   |
| 70           | 25                   |
| 80           | 25                   |
| 90           | 30                   |
| 109          | 35                   |
| 125          | 40                   |
| 170          | 55                   |

### 3.4. Upstream and downstream slopes

The upstream and downstream slopes are one of the effective parameters in the stability of the Rockfill and Embankment dams. The coarser the soil material, the steeper slope would be selected. The upstream slope of these dams also needs to be protected against damage from repeated wave impacts. In this research, dam upstream and downstream slopes were considered to be the same for all behavioral models, and materials related to the zoned areas were omitted to simplify. In each height class, three different cases of the dam upstream and downstream slopes were considered, as shown in Table 4. Thus, Case-1 represents the gentle slope and Case-3 denotes the steep slope where the letters "V" and "H" represent the vertical and horizontal dimensions respectively.

Table 4. Different cases of upstream and downstream slopes of dam models

| Slope Reference Code | Type | Downstream Slope (V:H) | Upstream Slope (V:H) | Description    |
|----------------------|------|------------------------|----------------------|----------------|
| Case-1               |      | 1: 2.5                 | 1: 2.5               | Gentle Slope   |
| Case-2               |      | 1: 2.0                 | 1: 2.0               | Moderate Slope |
| Case-3               |      | 1: 1.5                 | 1: 1.5               | Steep Slope    |

### 3.5. Asphalt concrete core types

The production of an appropriate asphalt concrete core requires proper design and production of the mixture, accurate weighing and transporting it so as not to cause premature separation or cooling, and ultimately gets good compaction.

The compaction is the last and critical step in the construction phase in which the final performance of the asphalt mixture as a sealing element depends on it. Insufficient compaction leaves a large volume of air cavities, which in turn increases the degree of permeability of the mixture. In addition, improper compaction reduces resistance and increases fatigue cracks.

After impounding, air cavities are replaced with water, which in cold weather is more likely to be damaged by the repeated freezing and thawing cycles. The construction of an asphalt concrete core of the rockfill dam, depending on both environmental conditions and the construction limits, as shown in Figure 1, can typically be accomplished by one of the following cases:

- Vertical core located in the center of the dam cross section (Central Core)
- Stable inclined core that deviates from the dam heel to the upstream side (Inclined Core)

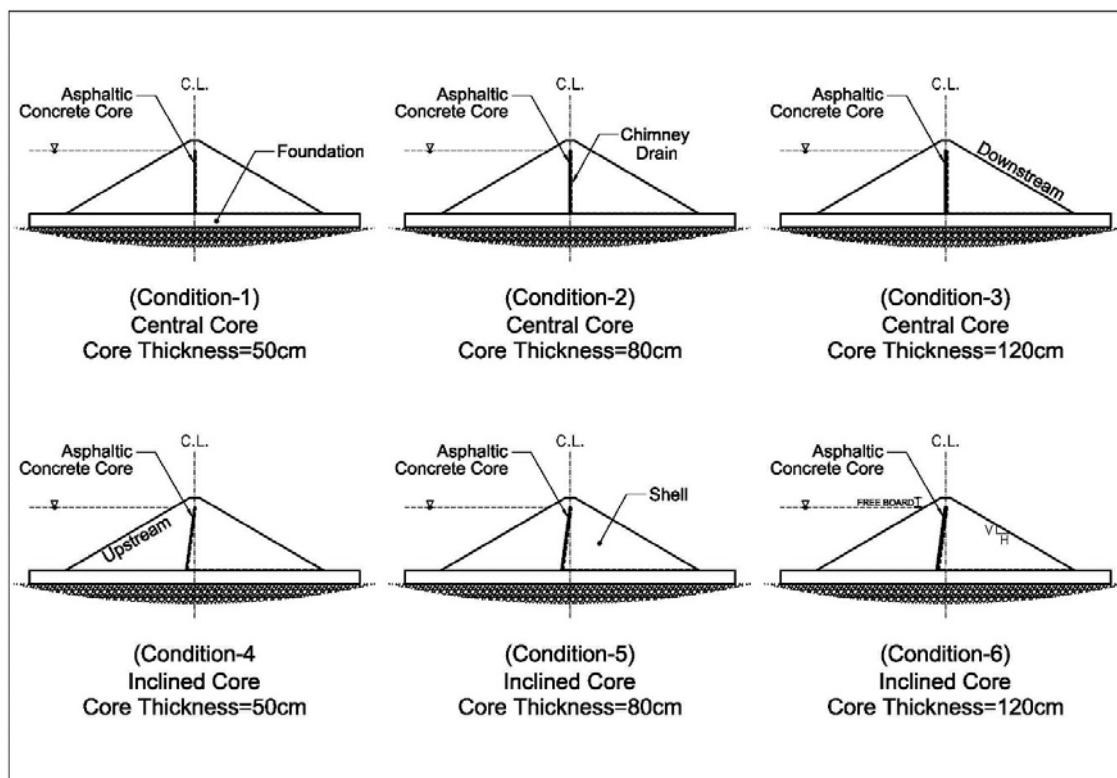


Figure 1. Thickness and the position of the asphalt concrete core

The central asphalt concrete core is built usually in dams less than 60m high, while in dams with higher height, the top of the asphalt concrete core is inclined toward the downstream side to prevent the separation of the upstream fill from the core near the dam crest. Although an inclined core allows the transfer of

hydrostatic loads to the downstream fill, involve additional costs. Moreover, the construction of a central asphalt concrete core allows for possible repairs of the core by injection.

The minimum core thickness is usually recommended to be 50cm (Creegan & Monismith). In this study, for asphalt concrete cores, thicknesses of 50, 80, and 120cm in two core position types of vertical (V:H) 1:0 and inclined (V:H) 1:0.2 are assigned to behavioral models.

### 3.6. Construction and Impounding stages

The six cases mentioned in Section 3.5 were investigated in four different construction and impounding stages, as shown in Table 5.

Table 5. Construction and impounding stages

| Water Level Condition in Dam Reservoir | Status Reference Code |
|--|-----------------------|
| End of Construction                    | EOC                   |
| Steady State with Full Reservoir       | SSF                   |
| Steady State with Half Full Reservoir  | SSH                   |
| Rapid Drawdown                         | RDD                   |

As can be seen in Figure 2, in the case of "Full Reservoir", the water reservoir behind the dam is full from the foundation to the maximum allowable height except for the freeboard. In the case of "Half Full Reservoir", the water level in the reservoir is half of that in the SSF. "End of Construction" is the stage when the dam is completely constructed but the impoundment has not started. "Rapid Drawdown", is a critical situation that may occur for a dam during which the reservoir water is suddenly drained.

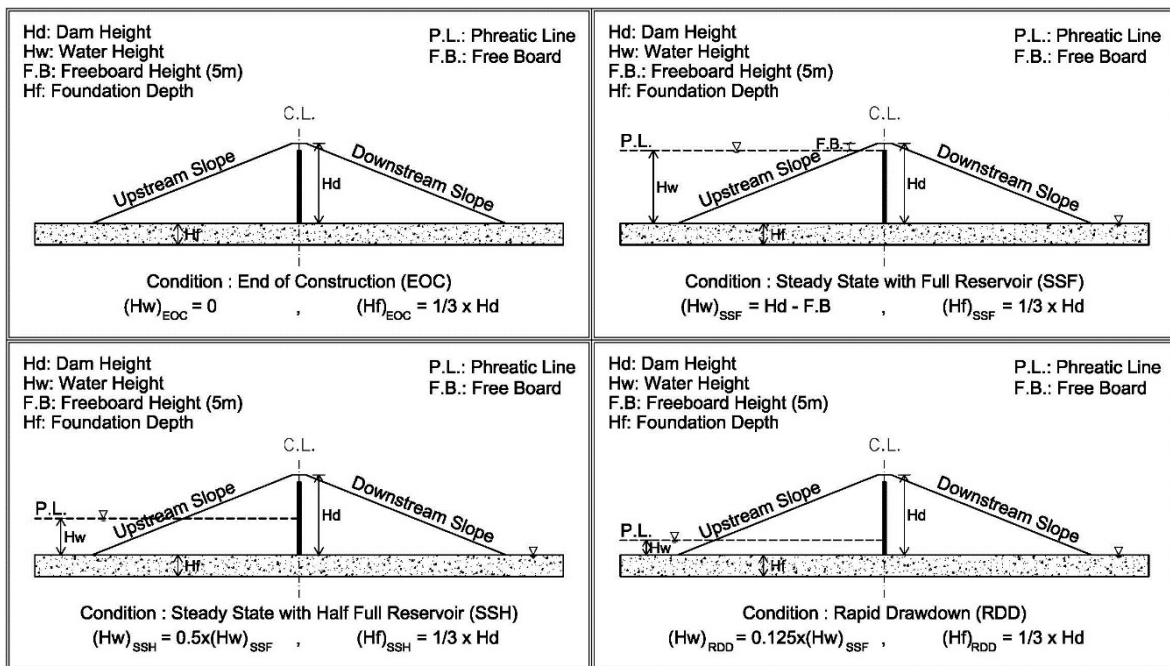


Figure 2. Different construction and impounding stages

In this paper, for RDD mode, the amount of water left in the reservoir was assumed to be one-eighth of the height in SSF mode. It is also very common to use a chimney drain in asphalt concrete core for the high Rockfill dams with different impounding stages in the reservoir (Cooper & Van Aller, 2004).

The chimney drain controls leakage and increases the stability of the downstream slope in different construction and impounding stages (Moayed et al., 2012). Due to the above-mentioned benefits, as shown in Figure 3, the

A chimney drain was used for all models. A chimney drain can reduce the pressure in a long vertical strip in the central part of the dam and increase the stability safety factor. Execution of the chimney drains at a relatively low cost would bring significant benefits. These drains generally pass a small volume of water through the dam due to the pressure of the dam body, so they do not even need much to get water out of the dam body (Höeg, 1993).

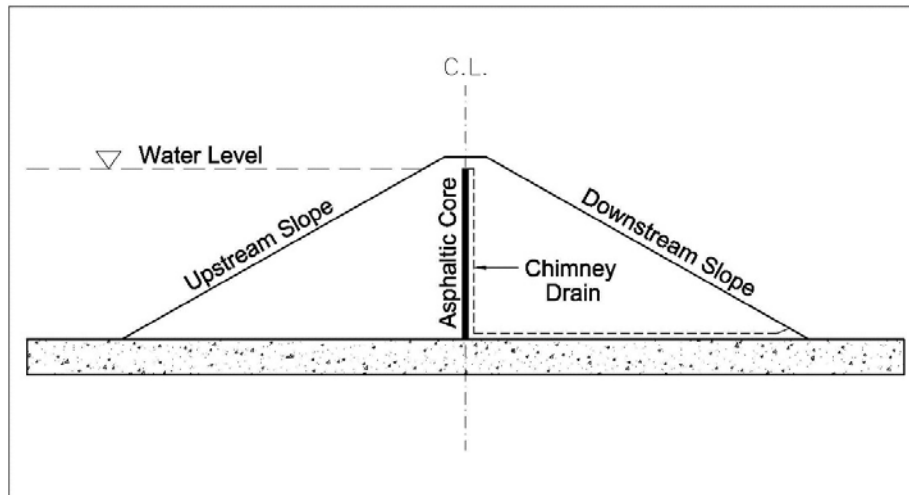


Figure 3. Chimney drain

## 4. MODELING

### 4.1. Boundary conditions

#### 4.1.1. Constraints Boundary conditions

In modeling, it is necessary to assign the type of support and the appropriate constraints boundary conditions to the models. In this way, the supports can be defined by restricting the displacements for each vertical or horizontal direction or both simultaneously. In this research, for all models, the lower boundary of the foundation was restricted in horizontal and vertical directions, so the foundation was not allowed to move in those directions. Given the necessity of modeling, as mentioned earlier, foundation edges are cut and infinite on both sides. Also, both unbounded boundaries on the sides of the foundation are restricted horizontally but are allowed to displace in the vertical direction. The constraints boundary conditions are shown in Figure 4.

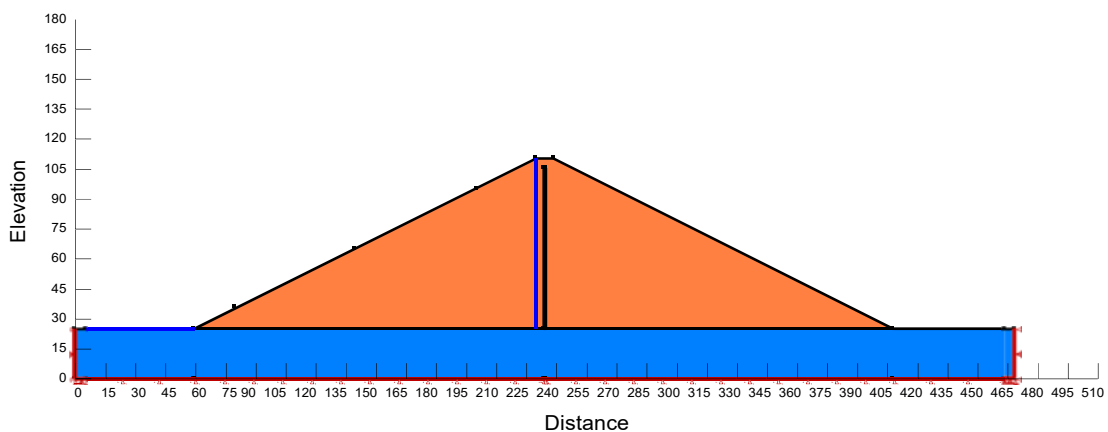


Figure 4. Constraints boundary conditions in both horizontal and vertical directions



#### 4.1.2. Reservoir water level boundary conditions

After reservoir impoundment, pressure from the water proportional to the reservoir water level height was exerted on both the dam body and its foundation, thus the mentioned pressure effects should be considered in the results. For this purpose, the water pressure should be defined as a kind of boundary condition to the affected surfaces. On the downstream side of the dam, the water level was defined based on the foundation, but since no water height was found on the foundation located on the downstream side of the dam, there were no boundary conditions in that part. Figure 8 shows the reservoir boundary conditions.

#### 4.2. Mesh size for Behavioral modeling

Given that the static stress-strain analysis was performed using the finite element method by SIGMA/W software, it is necessary to define an optimal pattern of mesh assigning to different zones of dam cross sections to achieve more accurate results. Therefore, In the first step, as an appropriate dam model, the simplified geometry of Styggevatn Dam located in Norway with 52 meters height from the foundation was studied as shown in Figure 5.

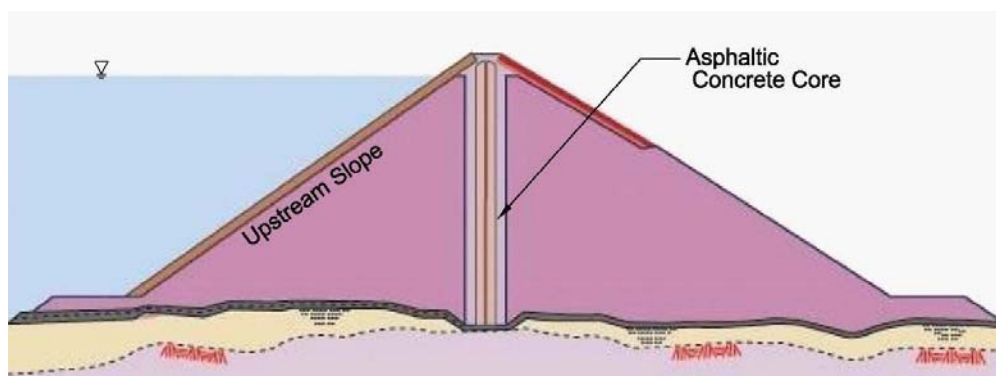


Figure 5. The Styggevatn Dam principal cross-section, located in Norway

In the second step, dam geometry was simplified so that toe drain, transition zones, shell zone, and details related to the asphalt concrete core connection to the foundation were not considered. Then, the coordinates of the constituent points of this model based on the real cross-section scale (Höeg, 1993) were obtained to enter SIGMA/W software. In the third step, to complete the modeling process, taking into account the dam height equal to 500mm, asphaltic core thickness equal to 50cm, same upstream and downstream slopes equal to 1.0:1.5 (V:H), and the foundation depth about one-third of the height i.e., 15m (Adikari, et.al, 1988), points were defined in the program and the special materials related to the core, shell, and foundation were assigned to them. In the last step, in order to determine the optimal mesh dimension based on a trial-and-error procedure, 10 numbers of mesh dimensions consisting of square elements and the integration order designated by the software as “4” were assessed. For this purpose, the 10 different dimensions mentioned above from 1m×1m to 10m×10m were applied to the model and after performing the analysis, in each case, the values of horizontal and vertical displacements at the points located on the dam crest were read according to Tables 6 and 7.

Table 6. Horizontal displacements for a specific point located on the dam crest

| Crest Point | Displacement (X-Direction) |        |        |        |        |        |        |        |        |         |
|-------------|----------------------------|--------|--------|--------|--------|--------|--------|--------|--------|---------|
|             | Mesh Dimension             |        |        |        |        |        |        |        |        |         |
|             | 1mx1m                      | 2mx2m  | 3mx3m  | 4mx4m  | 5mx5m  | 6mx6m  | 7mx7m  | 8mx8m  | 9mx9m  | 10mx10m |
|             | 0.0178                     | 0.0178 | 0.0179 | 0.0180 | 0.0180 | 0.0180 | 0.0179 | 0.0180 | 0.0181 | 0.0184  |

As shown in Figure 6, for one of the samples, the displacement vectors showed the state of horizontal displacement depending on the different mesh conditions.

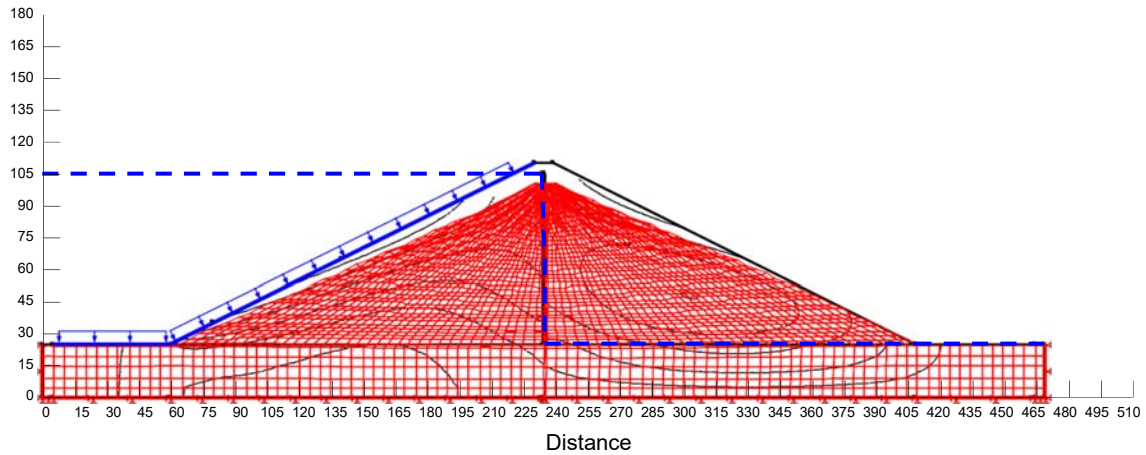


Figure 6. Horizontal displacement vectors for height class 80 in full reservoir stage

Table 7. Vertical displacements for a specific point located on the dam crest

As depicted in Figure 7, for one of the samples, the displacement vectors showed the state of vertical displacement depending on the different mesh conditions.

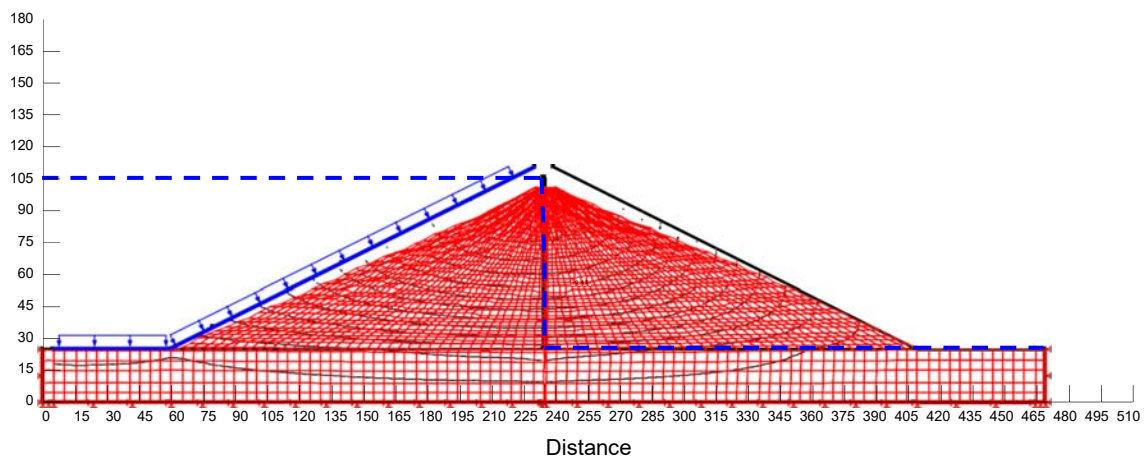


Figure 7. Vertical displacement vectors for height class 80 in full reservoir stage

As shown in the Tables and Figures above, the vertical and horizontal displacements in the range of mesh with elements 4, 5, and 6m had shown very little growth in change so, with an adequate approximation, the values of this range can be assumed to be constant. Therefore, the intermediate mesh size, i.e., 5.5m, is selected as the mesh dimensions as rectangular grid of quads and with the integration order designated by the software as “4”, to affect all models. Figure 8 shows the constraints boundary conditions, how to exert water pressure on the upstream side of the dam, and the mesh dimensions of 5mx5m.

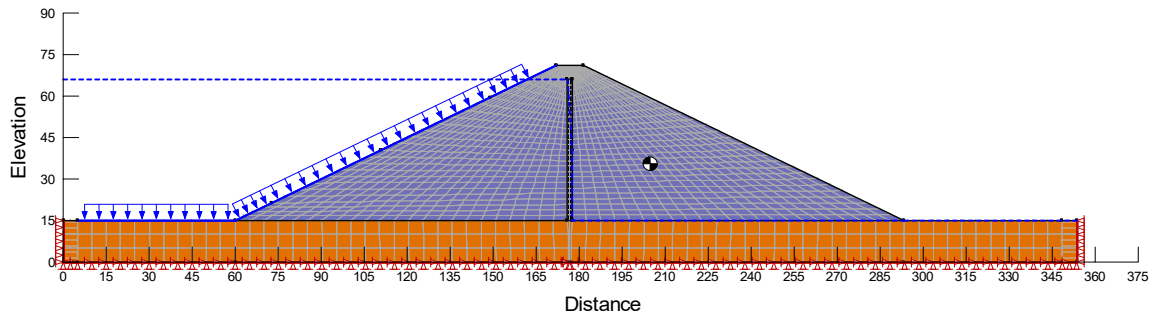


Figure 8. Constraints Boundary conditions, Water pressure on upstream and dam cross-section mesh

### 4.3. Assumptions of the static stress-strain analysis

In this study, according to the dams modeled by other researchers, the Earthfilling of the dam body has been assumed in one step for all models. Also, as one of the most important assumptions, for all conditions of impounding, the water level at the dam downstream side was placed on the foundation level. Due to a small variation in strain values in the asphalt concrete core, the behavior of the core material with an acceptable approximation can be assumed to be elastic (Adikari et al., 1988). In order to estimate the values of the geomechanical properties of foundation, shell, and core materials, the values used by previous researchers in similar cases were used using the Mohr-Coulomb theory according to Table 8. The type of analysis was considered load-deformation.

Table 8. Geomechanical properties of materials

| Dam Zone                | Unit Weight                   | Elastic Modulus | Poisson's Ratio | Cohesion Coefficient   | Internal Friction Angle |
|-------------------------|-------------------------------|-----------------|-----------------|------------------------|-------------------------|
|                         | $\gamma$ (kN/m <sup>3</sup> ) | C (kPa)         | $\nu$           | E (kN/m <sup>2</sup> ) | (°)                     |
| Shell                   | 22                            | 100000          | 0.25            | 40                     | 43                      |
| Asphaltic Concrete Core | 24                            | 200000          | 0.45            | 360                    | 28                      |
| Bedrock                 | 22                            | 200000          | 0.40            | 350                    | 35                      |

In the static analysis, the water unit weight of volume was equal to 9.807 kN/m<sup>3</sup> and according to a constant consideration of weather for all models, the atmospheric pressure value was considered as 101.33 kPa.

### 4.4. Evaluation of the specified points on the upstream slope

As shown in Figure 9, three specified points on the dam's upstream slope were considered. After performing the static stress-strain analysis, the obtained results from stresses, strains, and displacements of the specified points mentioned above were evaluated. In this way, the distances between those three points were selected so that each of them can be compared as a representative of the middle, upper and lower parts of the upstream slope. The upper point "T" was approximately one-ninth of the length of the upstream slope from the crest, and the lower point "B" was about the same distance from the foundation. The point "M" was in the middle of the upstream slope. Also, the point "T" has been selected so that in the SSF condition, it was below the water level for all models.

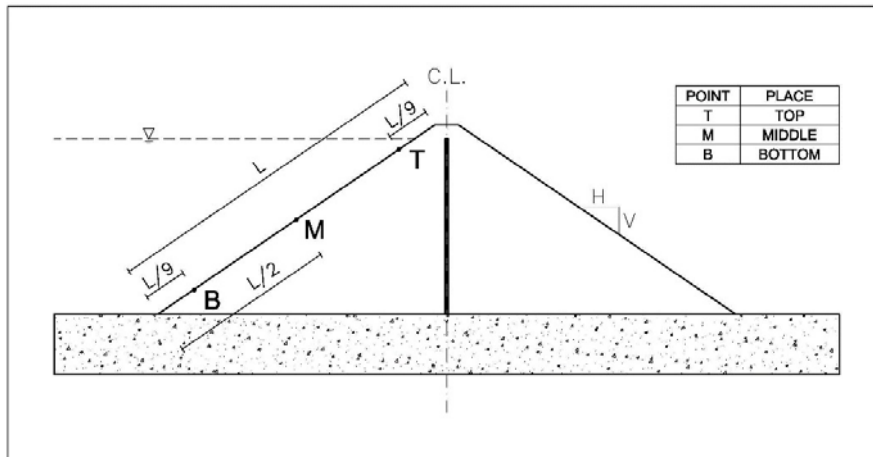


Figure 9. Upper, middle, and lower specified points on the upstream slope.

## 5. RESULTS

After performing the static stress-strain analysis, assessing and comparing the results, the maximum values of the total stress, strain, shear strain, deviator stress, shear stress, deviator strain, volumetric strain, and vertical and horizontal displacements at specified points (T, M and B) on the upstream slope were obtained for three slope cases (Case-1 ~ Case-3) and the four different construction and impounding stages. The results are shown in the following graphs. Our results demonstrated that with increasing the dam height, maximum total stress was increased for all construction and impounding stages for the upper, middle, and lower points and by reducing the slope, the maximum total stress decreased. Figure 10 shows a diagram of the maximum total stress at the middle-specified point “M” on the upstream slope in terms of the dam height at a slope of 1:1.5 (Case-3) and the EOC stage.

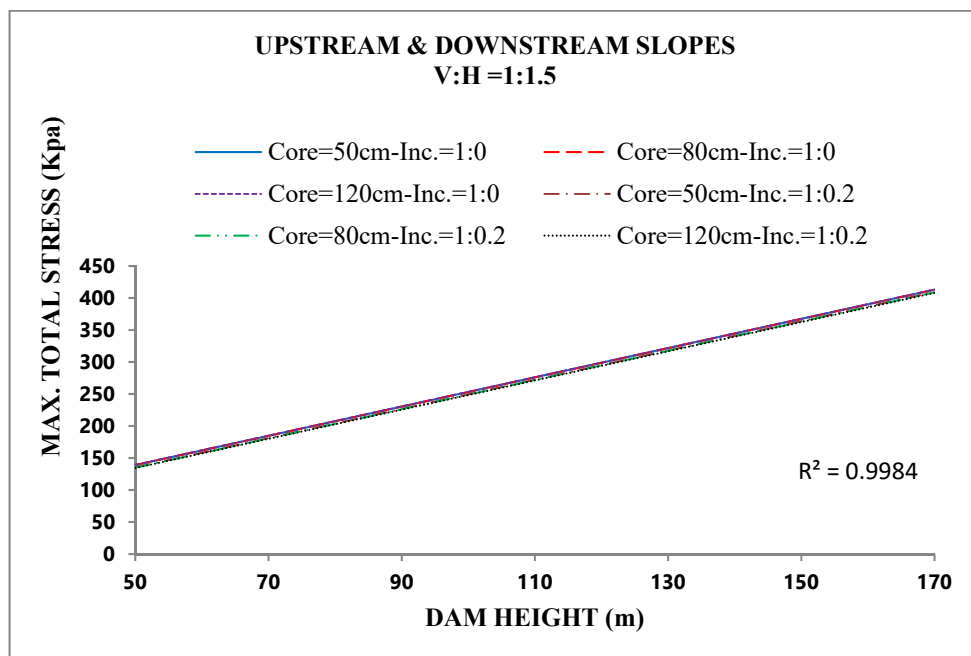


Figure 10. Maximum total stress diagram at the upstream middle point in terms of dam height

At specified points on the upstream slope, the maximum strain value increased with increasing height for all construction and impounding states. Figure 11 shows a diagram of the maximum strain at the middle point “M” on the upstream slope in terms of dam height at a slope of 1:2.5 (Case-1) and the EOC stage.

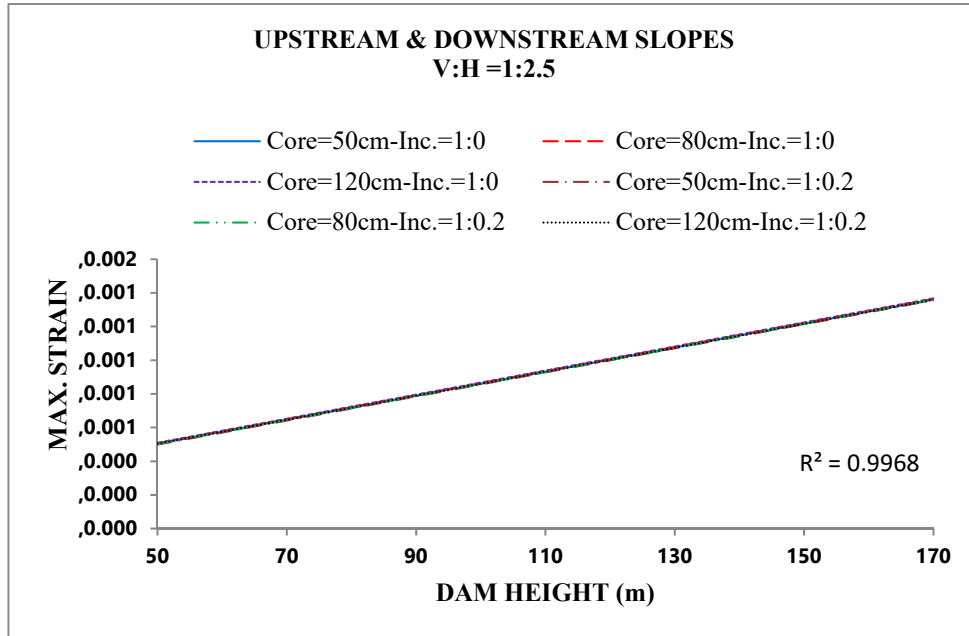


Figure 11. Maximum strain diagram at the upstream middle point in terms of dam height

In the upper, middle, and lower points, the maximum shear strain increased for all construction and impounding conditions as the height increased. Figure 12 shows a diagram of the maximum shear strain at the upper point “T” in terms of dam height, at a slope of 1:1.5 (Case-3) and the RDD stage.

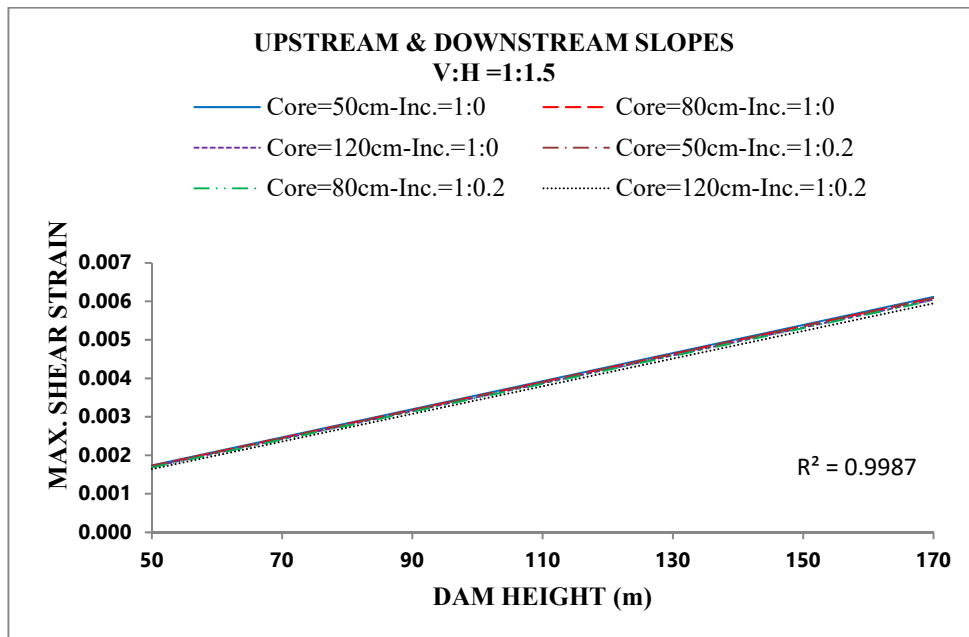


Figure 12. Maximum shear strain diagram at the upstream top point in terms of dam height

As the height increased, the value of deviator stress increased for all the specified points and all construction and impounding states. Figure 13 displays a diagram of the maximum deviator stress at the lower point “B” in terms of the dam height at a slope of 1:1.5 (Case-3) and the SSH stage.

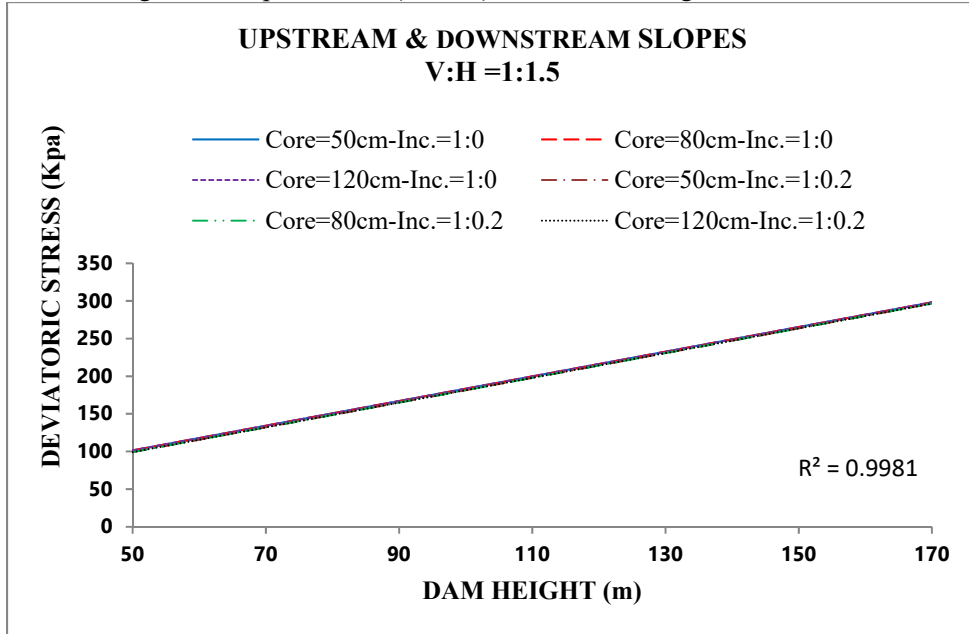


Figure 13. Maximum deviator stress diagram at the upstream bottom point in terms of dam height

For the specified points at the top, middle, and bottom of the rockfill dam upstream slope, the maximum shear stress increased for all construction and impounding conditions as the height increased. Moreover, with increasing the thickness of the asphalt concrete core, the value of maximum shear stress decreased in the full reservoir (SSF) and increased in other cases. Figure 14 shows a diagram of the maximum shear stress at the upper point “T” on the upstream slope in terms of dam height at a slope of 1:2.0 (Case-2) and the SSF stage.

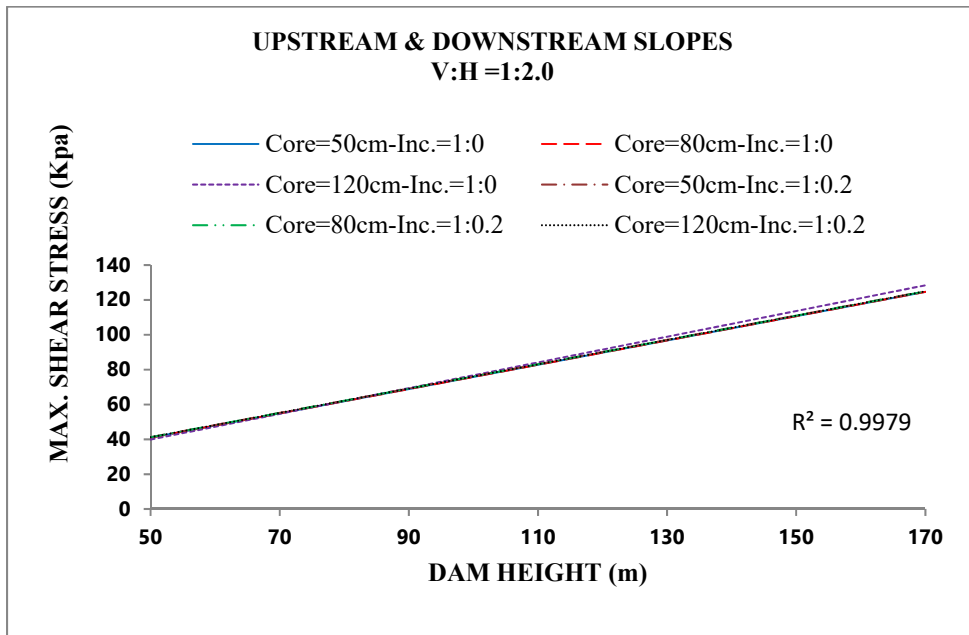


Figure 14. Maximum shear stress diagram at the upstream upper point in terms of dam height

A behavioral comparison of the numerical models against the forces acting on a structure showed that in the upper, middle, and lower points, as the height increased, the horizontal displacements were increased for all construction and impounding states. Figure 15 shows a diagram of the horizontal displacement at the middle point “M” on the upstream slope concerning the height of the dam at a slope of 1:2.0 (Case-2) and the SSH stage.

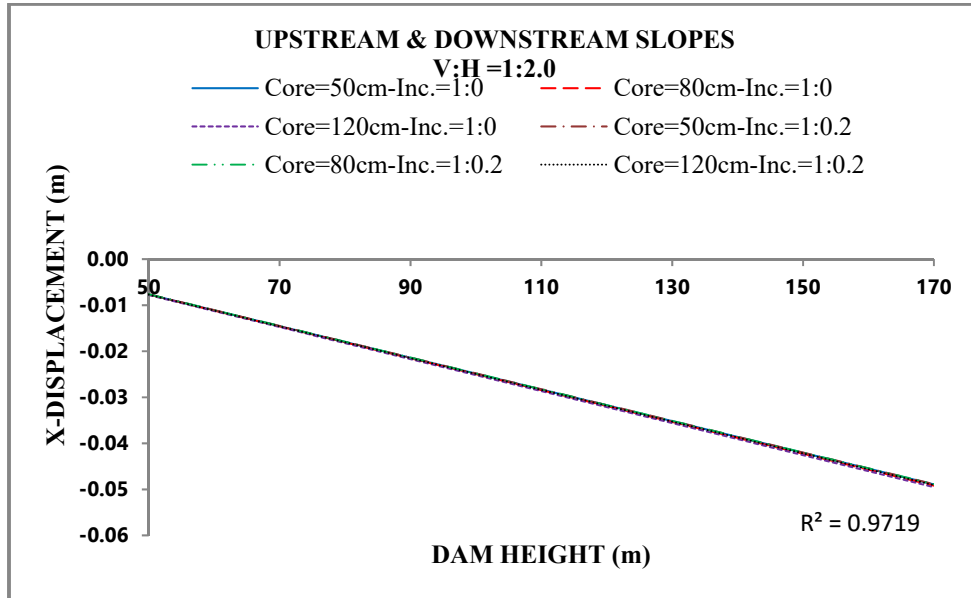


Figure 15. Horizontal displacement diagram at the upstream middle point in terms of dam height

As the height increased, the maximum deviator strain increased for all operation stages and all specified points on the upstream slope. Figure 16 shows a diagram of the maximum deviator strain at the lower point “B” in terms of the height parameter of the dam at a slope of 1:2.0 (Case-2) and the RDD stage.

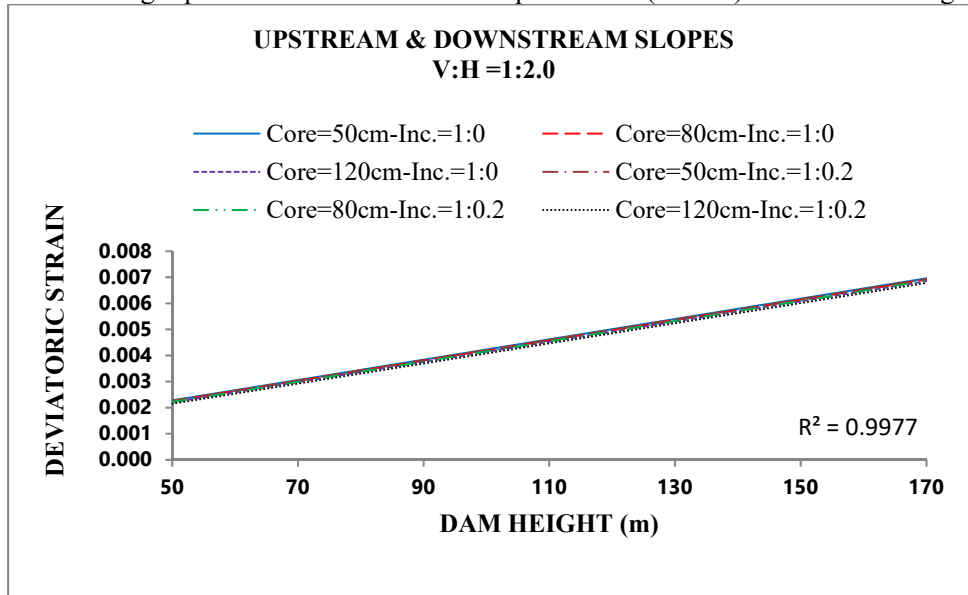


Figure 16. Maximum deviator strain diagram at the upstream lower point in terms of dam height

For three specified points mentioned above, increasing the height parameter causes increasing the vertical displacement values for all construction and impounding conditions. Figure 17 shows a diagram of the vertical displacements at the upper point of the upstream slope “T” concerning the height of the dam at a slope of 1:2.5 (Case-1) and the SSH stage.

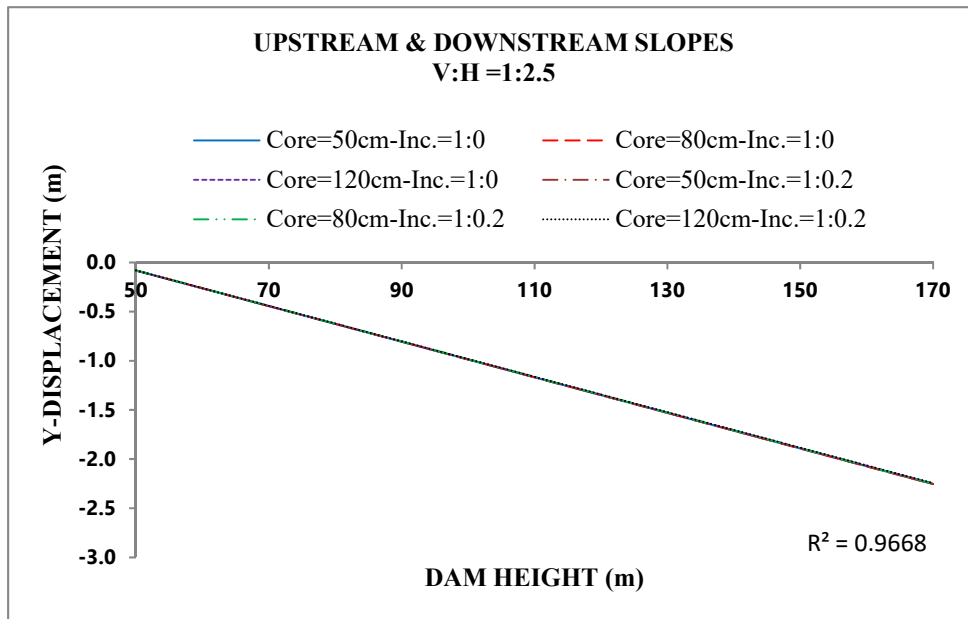


Figure 17. Vertical displacement diagram at the upstream top point in terms of dam height

For the specified points at the top, middle, and bottom of the rockfill dam upstream slope, the value of volumetric strain increased for all construction and impounding states as height increased. Figure 18 shows a diagram of the volumetric strain at the lower point of the upstream slope “B” in terms of the dam height, at a slope of 1:2.5 (Case-1) and the SSF stage.

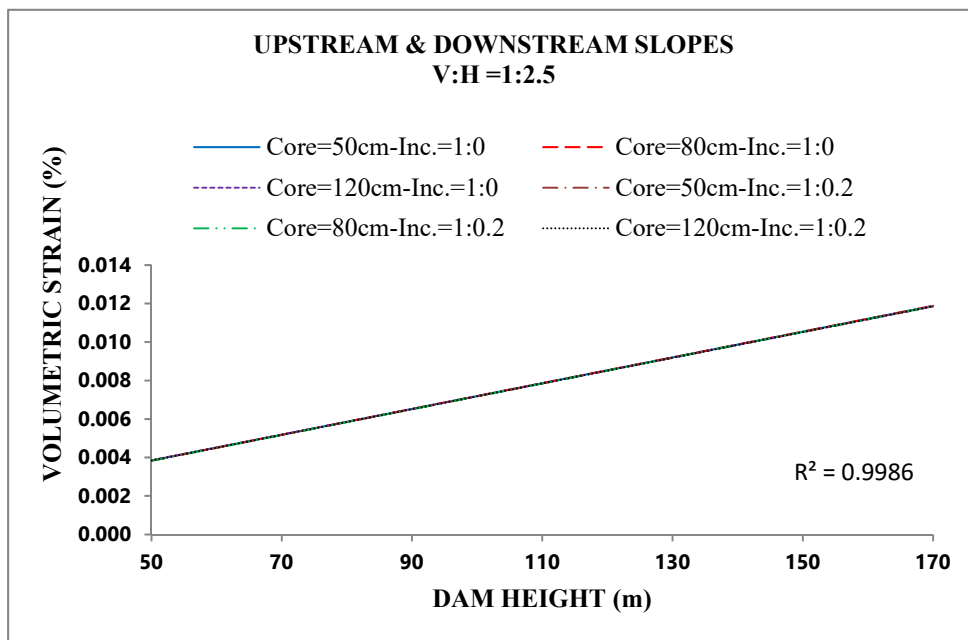


Figure 18. Volumetric strain diagram at the upstream bottom point in terms of dam height

Regarding other results of the points specified in the upstream slope of the dam models, some results were presented in terms of the location of points and accordance with the operating conditions and changes in



geometric parameters, especially slope conditions and asphaltic concrete core thickness in the conclusion section.

## 6. CONCLUSIONS

In addition to the general results presented in the comparative diagrams of upstream slopes, other results were presented in detail as follows:

### 6.1. Results obtained from the upper point specified on the upstream slope of the dam models (Point "T")

- As the slope became steeper, the maximum values of the strain, stress, shear stress, shear strain, deviator stress, deviator strain, and the volumetric strain were increased for all construction and impounding conditions.
- As the slope became steeper, the vertical displacement value decreased and the horizontal displacement value increased for all construction and impounding stages.
- As the thickness of the asphalt concrete core increased, the values of maximum shear strain, maximum strain, and maximum total stress were reduced for all construction and impounding conditions.
- As the thickness of the asphalt concrete core increased, the value of the maximum shear strain increased in the SSF stage, but the mentioned items decreased in other stages of construction and impounding.
- As the thickness of central and inclined asphaltic cores increased, the horizontal and vertical displacements decreased for all construction and impounding states.

### 6.2. The results obtained from the middle point specified on the upstream slope of the dams (Point "M")

- As the thickness of the asphalt concrete core increased, the maximum values of total stress, strain, and shear strain decreased in the SSF stage but increased in other states .
- As the thickness of central and inclined asphaltic cores increased, the horizontal displacement value decreased in the SSF stage and increased in other stages.
- As the central core thickness increased, the vertical displacement increased. Also, the vertical displacement decreased as the inclined asphaltic core thickness increased.
- As the slope became steeper, in the EOC stage, the maximum values of strain, stress, shear stress, shear strain, deviator stress, deviator strain, volumetric strain also vertical and horizontal displacements increased for all construction and impounding conditions.
- In the steeper slope, in the RDD stage, the maximum values of strain, stress, shear stress, and shear strain along with the deviator stress, deviator strain, and volumetric strain increased, the vertical displacement became bigger, and the horizontal displacement becomes smaller.
- In a steeper slope, in the SSF stage, the maximum values of strain, shear stress, and shear strain, along with the volumetric strain, deviator stress, and deviator strain reduced, the maximum total stress increased, and finally the vertical and horizontal displacements became bigger.
- As the slope became steeper, in the SSH stage, the maximum values of strain, shear stress, shear strain, total stress along with the deviator stress, deviator strain, and volumetric strain decreased. Also on steeper slopes, the vertical displacement became smaller but the horizontal displacement became bigger.

### 6.3. The results obtained from the lower point specified on the upstream slope of the dams (Point "B")

- For dam models with the central core, with increasing the asphalt concrete core thickness, the maximum value of shear strain in the EOC and RDD stages increased but the mentioned items decreased for models with the inclined core. For models with a central core maximum shear strain in both the SSF and SSH stages was less than that for models with the inclined asphaltic core.

- As the thickness of the asphalt concrete core increased, the maximum values of total stress and strain reduced for all construction and impounding stages, but the horizontal and vertical displacements increased.
- As the thickness of the central core increased, in the SSH stage, the horizontal displacement decreased but the items increased in other states.
- As the thickness of the inclined core increased, the horizontal displacement decreased in the EOC and RDD stages, but the items increased in other impounding stages.
- As the slope became steeper, in the EOC stage, the maximum amounts of strain, stress, shear stress, shear strain, along with deviator stress, deviator strain, volumetric strain, and also the vertical and horizontal displacements increased for all construction and impounding stages.
- For points "M" and "B", as the slope became steeper, in the SSF stage, the maximum values of strain, shear stress, shear strain, along with the deviator stress, deviator strain, and the volumetric strain reduced, but in the mentioned stage, the maximum total stress and displacements in both vertical and horizontal directions increased.
- For points "M" and "B", as the slope became steeper, in the SSH stage, the maximum values of the strain, shear stress, shear strain, along with the deviator stress, deviator strain, volumetric strain, and maximum total stress reduced. In the mentioned stage, the vertical displacement became smaller but the horizontal displacement became bigger.

## REFERENCES

Adikari, G. N., Valstad, T., Kjoernsli, B., & Hoeg, K. (1988). Behaviour of Storvatn Dam, Norway: a case of prediction versus performance. *Publikasjon-Norges Geotekniske Institutt*(173), 1-8.

Baziar, M. H., Salemi, S., & Heidari, H. (2006). Analysis of Earthquake Response of an Asphalt Concrete Core Embankment Dam. *International Journal of Civil Engineering*,

Cooper, C. R., & Van Aller, H. W. (2004). Best practices for conduits through embankment dams. *Proceedings ASDSO Dam Safety*.

Creegan, P. J., & Monismith, C. L. (1996). Asphalt-concrete water barriers for embankment dams.

Feizi, S., Mirghasemi, A. A., & Ghanooni, SH. (2005). Static and dynamic investigation of the behavior of rockfill dams with asphalt concrete cores in three-dimensional condition. 1<sup>st</sup> National Congress of Civil Engineering. *Sharif University of Technology*.

Gatmiri, B., & Mokarram, N. (2003). Dynamic Analysis of Asphaltic Concrete Core Embankment Dams. 4th. International Conference on Seismology and Earthquake Engineering.

Höeg, K. (1993). Asphaltic concrete cores for embankment dams. *Norwegian Geotechnical Institute Publicatie*.

Ltd, G.-S. I. (2010). *Stress-Deformation Modeling with Sigma/W 2007 Version*.

Ltd., G.-S. I. (2010). *Stability Modeling with Slope/W 2007 Version*.

Mahinroosta, R. (2007). Seismic response of an asphaltic concrete core embankment dam: 4th International Conference on Earthquake Geotechnical Engineering.

Moayed, R. Z., Rashidian, V. R., & Izadi, E. (2012). Evaluation of Phreatic Line in Homogenous Earth Dams with Different Drainage Systems. *Civ. Eng. Dept. Imam Khomeini Int. Uni. Qazvin, Iran*.

Razmkhah, A., & Shiravi, S. (2016). Parametric Evaluation of the Static Stability Analysis of the Asphaltic Concrete Core Rockfill Dams. *Journal of Water Sciences Research*, 8(1), 51-62.

Valstad, T., Selnes, P. B., Nadim, F., & Aspen, B. (1992). Seismic response of a rockfill dam with an asphaltic concrete core. *Publikasjon-Norges Geotekniske Institutt*, 184.

Wu, Y., Jiang, X., Fu, H., Xu, K., & Wu, Z. (2018). Three-Dimensional Static and Dynamic Analyses of an Asphalt-Concrete Core Dam.

Moayed, R. Z., & Fatemi, M. (2001). Static Stress-Strain Analysis of the Asphalt Concrete Core Embankment Dams: 4<sup>th</sup> Conference on Dam Construction, IRCOLD, Tehran.

Kjaernsli, B., Valstad, T., & Hoeg, K. (1991). *Rockfill Dams*, N.G.I.